

On the impact of the Higgs boson on the production of exotic particles at the LHC

A. G. Hessler, A. Ibarra, E. Molinaro and S. Vogl

*Physik-Department T30d, Technische Universität München,
James-Frank-Straße, 85748 Garching, Germany.*

Abstract

Many new physics models contain new particles that interact with the Higgs boson. These particles could be produced at the LHC via gluon-gluon fusion with an off-shell Higgs and, if charged under a gauge group, also via gluon-gluon fusion with an off-shell Z boson and the Drell-Yan process. We consider in this paper simplified scenarios where the Standard Model is extended by one scalar or fermionic field that interacts with the Higgs boson and we evaluate the impact of the Higgs interaction on the production of the exotic particles at the LHC. This analysis applies in particular to TeV scale seesaw scenarios of neutrino mass generation.

1 Introduction

The discovery by the ATLAS and CMS collaborations of a new boson with a mass of approximately 125 GeV has opened a new era in Particle Physics [1, 2]. On the one hand, the measured properties of the new bosonic particle are in remarkable agreement with those expected for the long-awaited Higgs boson [3], predicted by the mechanism of spontaneous breaking of the electroweak symmetry to generate the gauge boson, charged lepton and quark masses. On the other hand, the discovery of the new boson also constitutes evidence for a new fundamental interaction in Nature. From the theoretical point of view, this new interaction plays a crucial role in preserving the perturbative unitarity of the theory at high energies and in guaranteeing the renormalizability of the Standard

Model (SM). However, it also has many phenomenological implications, such as the imprint it leaves in the electroweak precision measurements which led to indirect hints for the existence of the Higgs boson already in the LEP era [4], or its production at the LHC and decay into other particles, that led to its identification.

New particles beyond the SM could also couple to the Higgs field. More specifically, the gauge and the Lorentz symmetries allow interaction terms of the Higgs doublet H with new scalars S_i of the form $|H|^2|S_i|^2$, among other terms, or with fermions Ψ_1, Ψ_2 of the form $\bar{\Psi}_1\Psi_2 H$. We consider for simplicity a minimal number of new degrees of freedom in addition to the SM, that is we explicitly analyse the production in proton-proton colliders of new particles in models with just one extra $SU(2)_L$ scalar multiplet or one new chiral fermion. Under these assumptions, it can be checked that the scalar Higgs portal term is present in the potential for any assignment of the gauge quantum numbers for the scalar field, while the fermionic Higgs portal term exists only if either Ψ_1 or Ψ_2 is one SM lepton and the new chiral fermion has gauge quantum numbers under $SU(3)_c \times SU(2)_L \times U(1)_Y$ equal to $(1, 1, 0)$ or $(1, 3, 0)$ (these two cases correspond to the renowned type I [5] and type III [6] seesaw mechanisms, respectively). Thus new scalars or fermions can be produced at the LHC via their electroweak gauge interactions with the partons inside the protons (see, *e.g.*, [7, 8, 9]). However, this is not the only possibility for production, since the newly discovered Higgs particle can also mediate the production of exotic scalars or fermions. Due to the fairly good recent determination of the mass and some of the couplings of the Higgs boson, a quantitative analysis of the impact of the Higgs boson on the production rate of exotic particles at the LHC has now become possible. Therefore, we perform in this work a quantitative comparison between Higgs-mediated channels and the well-known electroweak production channels. To the best of our knowledge, such a systematic analysis has not been done before.

The paper is organized as follows: In section 2 we recapitulate basic elements of the formalism to calculate the production cross-section of exotic particles at the Large Hadron Collider. In section 3 we study the production of exotic scalars, while in section 4 the production of exotic fermions is analyzed, considering in both sections a center-of-mass energy of 8 and 14 TeV. In section 5 we briefly comment on the prospects to observe exotic particles in a hypothetical proton-proton collider operating at a center-of-mass energy of 100 TeV and, lastly, in section 6 we present our conclusions.

2 Heavy particle production at the LHC

New physics states interacting with the Higgs boson can be produced at the LHC via the gluon-gluon fusion (ggF) vertex with a Higgs particle.¹ The leading order contribution to this vertex consists of a triangular diagram with the top quark in the loop and subleading corrections due to the bottom quark, while lighter flavours are essentially negligible. We follow the common procedure in the literature [10] and take the gluon-gluon-Higgs (ggH) process into account by introducing an effective Lagrangian for the Higgs interaction with gluons

$$\mathcal{L}_{\text{H,eff}} = \frac{1}{4} G_H G_{\mu\nu}^a G^{a\mu\nu} \frac{h}{v}, \quad (1)$$

where G_H is an effective coupling and $v \simeq 246$ GeV is the Higgs vacuum expectation value (vev), while $G_{\mu\nu}^a$ and h correspond to the gluon field strength tensor and the Higgs field respectively.

The effective coupling can be determined by matching the amplitude of the effective theory to the corresponding amplitude in the SM and is given, keeping only the contribution of the top quark, by

$$G_H = \frac{\alpha_S}{2\pi} \left| F_H \left(\frac{4m_t^2}{P^2} \right) \right|, \quad (2)$$

where α_S is the strong coupling constant and F_H corresponds to the well-known triangle form factor [12] which depends on the top quark mass $m_t = 173.5$ GeV and the momentum scale of the process P . Depending on whether the process considered is on-shell Higgs production or new physics production from a Higgs boson at arbitrary virtuality, the scale P is either set by the Higgs mass $m_h \simeq 125$ GeV or by the total partonic center-of-mass (c.o.m.) energy $\sqrt{\hat{s}}$. The form factor can be calculated analytically and is given by

$$F_H(\tau) = \tau [1 + (1 - \tau) f(\tau)], \quad (3)$$

with

$$f(\tau) = \begin{cases} \arcsin^2 \frac{1}{\sqrt{\tau}} & \text{if } \tau \geq 1 \\ -\frac{1}{4} \left[\log \left(\frac{1 + \sqrt{1 - \tau}}{1 - \sqrt{1 - \tau}} \right) - i\pi \right]^2 & \text{if } \tau < 1. \end{cases} \quad (4)$$

Furthermore, an additional contribution to gluon-gluon fusion can arise from the gluon-gluon- Z (ggZ) triangle diagram². Since we are only interested in the production

¹We will not consider here the production via vector boson fusion, although this process could give a non-negligible contribution to the cross-section at large momentum transfer [11].

²Furry's theorem forbids the analogous process with an intermediate photon.

from real on-shell gluons in the initial state, the general form of the ggZ vertex originally derived in [13] can be simplified and the effective Lagrangian reads

$$\mathcal{L}_{Z,\text{eff}} = \frac{1}{4} G_Z \partial_\alpha Z^\alpha G_{\mu\nu}^a \tilde{G}^{a\mu\nu}, \quad (5)$$

where $\tilde{G}^{\mu\nu}$ is the dual of the field strength tensor. The effective coupling G_Z is given by [14]

$$G_Z = \frac{\alpha_s}{2\pi} \frac{e}{s_w c_w} \left| \sum_Q (-1)_Q F_Z(\hat{s}, m_Q^2) \right|, \quad (6)$$

where s_w and c_w correspond to the sine and the cosine of the Weinberg angle, while the form factor reads

$$F_Z(\hat{s}, m_Q^2) = \frac{1}{\hat{s}} \left\{ 1 + \frac{2m_Q^2}{\hat{s}} \int_0^1 \frac{dx}{x} \log \left[1 - \frac{\hat{s}}{m_Q^2} x(1-x) \right] \right\}. \quad (7)$$

The sum runs over all quark flavours Q present in the triangle loop and $(-1)_Q$ equals $+1$ for up-type quarks and -1 for down-type quarks. The first term in the form factor in Eq. (7) is flavour-independent and therefore drops out once the sum over complete generations of quarks is performed. As the second term is proportional to the square of the quark mass, the top contribution will be once again dominant and lighter quark flavours can be safely neglected.

With the effective couplings G_H and G_Z , the partonic cross-sections can be calculated in different models; the corresponding expressions for the production of exotic scalar and fermionic particles will be reported in sections 3 and 4. We point out that the Higgs- and Z -mediated gluon-gluon fusion amplitudes do not interfere due to their different Lorentz index structure.

At the LHC, the production cross-section of the final state $X_1 X_2$, where X_1 and X_2 are not necessarily different particles, is the result of the convolution of the partonic cross-section with the corresponding parton distribution functions (PDFs) (see *e.g.* [11]). More specifically for the case of gluon-gluon fusion,

$$\sigma(pp \rightarrow X_1 X_2; s) = \int_{\tau_s}^1 \frac{d\mathcal{L}^{gg}}{d\tau} \sigma(gg \rightarrow X_1 X_2; \hat{s} = \tau s) d\tau, \quad (8)$$

where $\tau_s \equiv (m_{X_1} + m_{X_2})^2/s$, \sqrt{s} is the center-of-mass energy of the proton-proton collision and \mathcal{L}^{gg} is the gluon luminosity function, defined as

$$\frac{d\mathcal{L}^{gg}}{d\tau} = \int_\tau^1 \frac{g(x, \mu_F) g(\frac{\tau}{x}, \mu_F)}{x} dx. \quad (9)$$

The gluon PDF, $g(x, \mu_F)$, depends on the fraction x of the proton momentum carried by the parton and on the factorization scale μ_F , which represents the scale at which

the matching between the perturbative calculation of the matrix elements and the non-perturbative part related to the parton distribution functions is performed. In our analysis we will focus on the leading order contributions to the production cross-section of exotic particles via gluon-gluon fusion, however, it should be borne in mind that higher order corrections to this production channel can significantly enhance the cross-section. For example, comparing leading order results to state-of-the-art calculations for single Higgs production [15], one finds $K \equiv \sigma_{\text{NNLO+NNLL}}/\sigma_{\text{LO}} \sim 3$ at 14 TeV.

The same final state can be generated via the Drell-Yan (DY) process, *i.e.* by the exchange of an off-shell photon and/or Z boson in the s -channel in a quark-antiquark collision. The corresponding production cross-section via this channel reads

$$\sigma(p p \rightarrow X_1 X_2; s) = \sum_{q=u,d} \int_{\tau_s}^1 \frac{d\mathcal{L}^{q\bar{q}}}{d\tau} \sigma(q\bar{q} \rightarrow X_1 X_2; \hat{s} = \tau s) d\tau, \quad (10)$$

where the quark luminosity function is

$$\frac{d\mathcal{L}^{q\bar{q}}}{d\tau} = \int_{\tau}^1 \frac{q(x, \mu_F) \bar{q}\left(\frac{\tau}{x}, \mu_F\right) + q\left(\frac{\tau}{x}, \mu_F\right) \bar{q}(x, \mu_F)}{x} dx, \quad (11)$$

with $q(x, \mu_F)$ and $\bar{q}(x, \mu_F)$ the quark and antiquark PDFs, respectively. The relative importance of the two production mechanisms depends on the details of the new physics model. In the following, we discuss separately the case of scalar particle production and of fermionic particle production.

3 Scalar multiplet production at the LHC

We consider a minimal extension of the SM with one additional complex scalar field S , assumed to be uncoloured, and which is a generic multiplet of $SU(2)_L$ with weak isospin T and hypercharge Y (we will not consider new particles which are charged under $SU(3)_c$ as their production is completely dominated by strong interactions). The scalar field S has $n = 2T + 1$ components, which are

$$S = (S_1, \dots, S_n)^T. \quad (12)$$

Then, all the interactions of S with the SM electroweak gauge bosons and the Higgs doublet H are given by the Lagrangian

$$\mathcal{L}_S = (D_\mu S)^\dagger (D^\mu S) - V(S, H). \quad (13)$$

In the charge basis the covariant derivative D_μ takes the usual form,

$$D_\mu = \partial_\mu - i \frac{g}{\sqrt{2}} (W_\mu^+ T^+ + W_\mu^- T^-) - i \frac{1}{\sqrt{g^2 + g'^2}} Z_\mu \left(g^2 T^3 - g'^2 \frac{Y}{2} \right) - i \frac{gg'}{\sqrt{g^2 + g'^2}} A_\mu Q,$$

where we define the electric charge $Q = T^3 + Y/2$.

We consider as benchmark scenario in our discussion the most generic renormalizable scalar potential $V(S, H)$ [16] invariant under a global $U(1)$ symmetry:³

$$\begin{aligned} V(S, H) = & \mu_H^2 H^\dagger H + f_1 (H^\dagger H)^2 + \mu_S^2 S^\dagger S + f_2 (S^\dagger S)^2 + f_3 (H^\dagger H) (S^\dagger S) \\ & + f_4 (H^\dagger \tau^a H) (S^\dagger T^a S) + f_5 (S^\dagger T^a S) (S^\dagger T^a S) . \end{aligned} \quad (14)$$

We define T^a (τ^a) for $a = 1, 2, 3$ as the generators of $SU(2)_L$ in a generic (the fundamental) representation, such that, in a basis in which T^3 is diagonal, $T^3 S_1 = T S_1$ and $T^3 S_n = -T S_n$.

After electroweak symmetry breaking, one of the components of S is neutral for particular choices of the weak isospin and the hypercharge. In the following, we assume that the neutral component of the scalar multiplet does not acquire a vev (or acquires only a very small vev, as in the examples that will be shown later), such that the formalism for the gluon-gluon fusion production mechanism described in section 2 can be applied.

The coupling f_4 in Eq. (14) controls the mass splitting of the multiplet components, at tree level.⁴ In the following, we will classify the multiplet components by the electric charge, where we refer to the component with charge equal to Q by $S^{(Q)}$. In this notation, the tree level squared mass of each eigenstate after electroweak symmetry breaking is given by

$$m_{S^{(Q)}}^2 = \mu_S^2 - \frac{1}{4} \Lambda_Q v^2, \quad (15)$$

where the coupling Λ_Q is defined as

$$\Lambda_Q = -2 f_3 + f_4 T^3 = -2 f_3 + f_4 \left(Q - \frac{Y}{2} \right), \quad (16)$$

and controls the strength of the interaction of the Higgs boson with two scalars, namely

$$\mathcal{L}_{\text{int}} = \frac{1}{2} \Lambda_Q v h S^{(Q)} \bar{S}^{(Q)} + \frac{1}{4} \Lambda_Q h^2 S^{(Q)} \bar{S}^{(Q)}. \quad (17)$$

Note that the mass splitting among the members of the multiplet, labelled by their electric charges, can be positive or negative depending on the sign of the quartic coupling f_4 .

³In the case of a real multiplet, the kinetic term in Eq. (13) is multiplied by a factor 1/2 and the operator $S^\dagger T^a S$ in Eq. (14) is identically zero, so that the components of a real multiplet are degenerate in mass.

⁴If the global $U(1)$ is explicitly broken to an accidental Z_2 symmetry, then for n even and $Y = 1$ the operator $(H^\dagger \tau^a \tilde{H})(S^\dagger T^a \tilde{S})$ is allowed, where \tilde{H} and \tilde{S} are the conjugate scalar multiplets. This operator provides an independent contribution to the relative mass splitting of the S components.

The parameter space spanned by the multiplet masses and couplings is constrained by various theoretical and phenomenological considerations, as we will briefly discuss now. Under the common requirement of vacuum stability, the following tree level conditions for the couplings must be fulfilled [16]:

$$f_{1,2} > 0, \quad (18)$$

$$\Lambda_Q < 4\sqrt{f_1 f_2} = 2 \frac{m_h}{v} \sqrt{2 f_2} \simeq 5, \quad (19)$$

where in the last equation the numerical value corresponds to the perturbativity limit $f_2 = 4\pi$.

Unitarity bounds on scalar-scalar and scalar-gauge boson scattering amplitudes constrain the couplings in the scalar potential. These constraints are model dependent and must be derived for each multiplet dimension and choice of hypercharge and $U(1)$ or Z_2 charge from the contributing process amplitudes involving the corresponding couplings. Constraints from tree level partial wave unitarity impose that $n \leq 8$ ($n \leq 9$) in the case of a complex (real) scalar multiplet (see, *e.g.*, [17]). Furthermore, electroweak precision constraints, which are usually formulated in terms of the so-called oblique parameters S , T and U [18], need to be taken into account. The most stringent constraint stems from the T parameter, while S and U provide weaker limits. Expressions for these in the case of an additional scalar multiplet of arbitrary size, which does not acquire a vacuum expectation value, have been calculated in [19]. Also, additional charged scalars coupled to the Higgs contribute to the $h \rightarrow \gamma\gamma$ rate [20]. Concerning the mass spectrum, the invisible width of the Z boson typically implies a lower bound, $m_{S^{(Q)}} \gtrsim m_Z/2 \simeq 45$ GeV.

Notice that a complex scalar multiplet can provide a viable dark matter candidate if it has a vanishing hypercharge –as dictated by direct detection constraints– and if its lightest component is neutral. Interestingly, in the case of a scalar multiplet of dimension $n \geq 7$ and $Y = 0$, the neutral component is naturally long lived, without imposing any additional global symmetry, because it is not possible to construct renormalizable or dimension-5 operators that would mediate decays into SM particles [21].

We finally remark here that our results also hold in the case in which the vev of the new multiplet is non-zero, provided it is much smaller than the electroweak scale. In this case the global $U(1)$ symmetry is only softly broken and the mixing between the neutral component of the multiplet and the Higgs boson is negligible. For example, this occurs in two-Higgs doublet models with an approximate global $U(1)$ symmetry, where a hierarchy between the vevs of the doublets, ϕ_1 and ϕ_2 , can be naturally achieved by adding to the scalar potential the term $\mu^2 \phi_1^\dagger \phi_2$, with $\mu \ll 1$ GeV, which softly breaks the global symmetry [22, 23]. Such explicit breaking of the symmetry can be avoided by

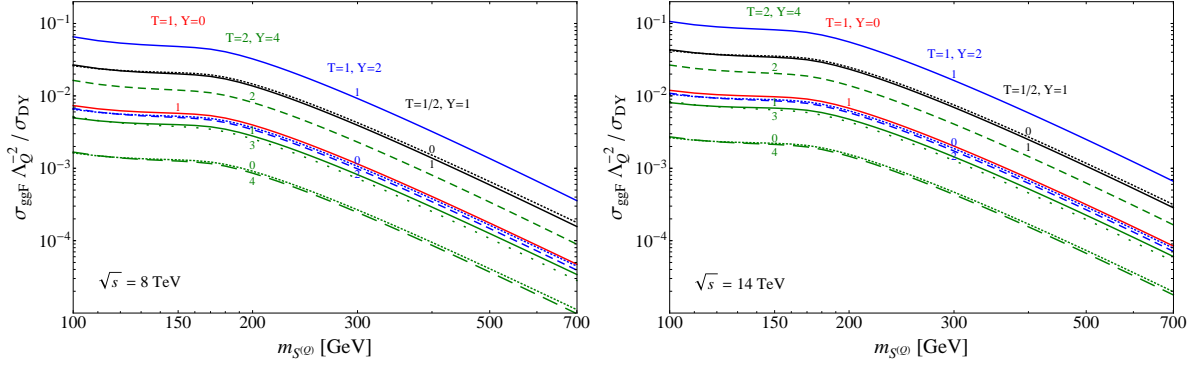


Figure 1: Relative contribution of the normalized gluon-gluon fusion vertex and the Drell-Yan production cross-sections as function of the scalar mass for 4 different $SU(2)_L$ multiplets, with $\sqrt{s} = 8$ TeV (left panel) and 14 TeV (right panel). The number on each line corresponds to the electric charge of the scalar particle.

the introduction of an additional scalar, say ϕ_3 , whose vev generates the required term: $\mu^2 = \mu' \langle \phi_3 \rangle$. As long as $\mu' \ll 1$ GeV, the minimum of the scalar potential corresponds to $\langle \phi_{2,3} \rangle \propto \mu' \ll \langle \phi_1 \rangle, \langle \phi_{3,2} \rangle$ [23] (see, *e.g.*, [24] for a concrete realization of this scenario). Similar considerations are valid in the Higgs triplet model, where S is in the adjoint of $SU(2)_L$ and has hypercharge $Y = 2$. This scenario is similar to the scalar part of the type II seesaw model for the generation of neutrino masses [25]. In this case the global symmetry is equivalent to the total lepton charge and it is explicitly broken by the term $\mu' H^T i \tau_2 S^\dagger H$ in the scalar potential. After the spontaneous breaking of the electroweak symmetry, the neutral component of the triplet takes a vev, $\langle S^0 \rangle \simeq \mu' v^2 / 2\mu_S^2 \ll v$. Indeed, an upper limit on $\langle S^0 \rangle$ is provided by the measurement of the ρ parameter, $\langle S^0 \rangle / v \lesssim 0.02$ or $\langle S^0 \rangle \lesssim 5$ GeV [26]. Similarly to the two-Higgs doublet model discussed above, the hierarchy between the vev of the triplet and the electroweak scale is possible because the scale μ' is naturally suppressed at all orders, due to the presence of a global (lepton number) symmetry.

The leading order ggZ cross-section for the production of a scalar-antiscalar pair vanishes [7], so that only Higgs-mediation is relevant here. The partonic cross-section with c.o.m. energy $\sqrt{\hat{s}}$ is

$$\sigma(gg \rightarrow S^{(Q)} \bar{S}^{(Q)}; \hat{s}) = \frac{\Lambda_Q^2 G_H^2 \sqrt{\hat{s}} \sqrt{\hat{s} - 4m_{S^{(Q)}}^2}}{4096 \pi (m_h^2 - \hat{s})^2}, \quad (20)$$

where the effective coupling Λ_Q is given in Eq. (16) and the gluon-gluon fusion effective coupling G_H is defined in Eq. (2).

On the other hand, the leading order Drell-Yan production cross-section of a scalar

pair for a generic multiplet of weak isospin T and hypercharge Y reads, for up-antiup quark collisions and neglecting the quark masses,

$$\begin{aligned} \sigma(u \bar{u} \rightarrow S^{(Q)} \bar{S}^{(Q)}; \hat{s}) = & \\ \frac{\pi \alpha_{\text{em}}^2 \hat{s} (1 - 4 m_{S^{(Q)}}^2 / \hat{s})^{3/2}}{288 c_w^4 s_w^4 (m_Z^2 - \hat{s})^2} & \left[4 Q^2 c_w^4 \left(\frac{16 m_Z^4 s_w^4}{9 \hat{s}^2} - 1 \right) + 4 \left(Q c_w^2 - \frac{2 Y s_w^2}{3} \right)^2 \right. \\ & \left. + \left(2 Q c_w^2 \left(1 - \frac{4 m_Z^2 s_w^2}{3 \hat{s}} \right) - Y \left(1 - \frac{8 s_w^2}{3} \right) \right)^2 + \frac{8}{3} Y^2 s_w^2 (c_w^2 - s_w^2) \right], \end{aligned} \quad (21)$$

while for the down-antidown quark initial state,

$$\begin{aligned} \sigma(d \bar{d} \rightarrow S^{(Q)} \bar{S}^{(Q)}; \hat{s}) = & \\ \frac{\pi \alpha_{\text{em}}^2 \hat{s} (1 - 4 m_{S^{(Q)}}^2 / \hat{s})^{3/2}}{288 c_w^4 s_w^4 (m_Z^2 - \hat{s})^2} & \left[4 Q^2 c_w^4 \left(\frac{4 m_Z^4 s_w^4}{9 \hat{s}^2} - 1 \right) + 4 \left(Q c_w^2 - \frac{Y s_w^2}{3} \right)^2 \right. \\ & \left. + \left(2 Q c_w^2 \left(1 - \frac{2 m_Z^2 s_w^2}{3 \hat{s}} \right) - Y \left(1 - \frac{4 s_w^2}{3} \right) \right)^2 + \frac{4}{3} Y^2 s_w^2 c_w^2 \right]. \end{aligned} \quad (22)$$

For charged scalar production, there is a contribution to the production cross-section both from photon and from Z boson exchange, hence the DY partonic cross-sections can be relatively enhanced or suppressed depending on the electric charge and weak isospin of each multiplet component. Notice that for $Y = 0$ and odd n the neutral component of the multiplet cannot be pair produced through electroweak interactions. The total production cross-section at the LHC is obtained by convoluting the single partonic cross-sections with the appropriate parton distribution functions, as described in section 2.⁵

We show in Fig. 1 the ratio between the gluon-gluon fusion cross-section σ_{ggF} normalized to the squared effective scalar coupling Λ_Q and the Drell-Yan production cross-section σ_{DY} for proton center-of-mass energies of 8 TeV (left panel) and 14 TeV (right panel). This quantity is, for a fixed $m_{S^{(Q)}}$, independent of the quartic couplings in the scalar potential and is determined exclusively by the electroweak quantum numbers of the scalar multiplet, as can be checked from Eqs. (20-22). The overall cross-section for each production mechanism is calculated using Eqs. (8-11) and (20-22) for several $SU(2)_L$ representations with fixed hypercharge. The numbers on each line represent the electric charge of the scalar mass eigenstate. In the numerical computation we use the CTEQ6 PDFs [28] and we fix both the factorization scale μ_F and the renormalization scale of the strong coupling constant at the invariant mass of the final state. As is noticeable from the plot, the dependence of the Higgs-mediated production cross-section with the

⁵The numerical results have been checked against a computation using CalcHEP 3.4 [27].

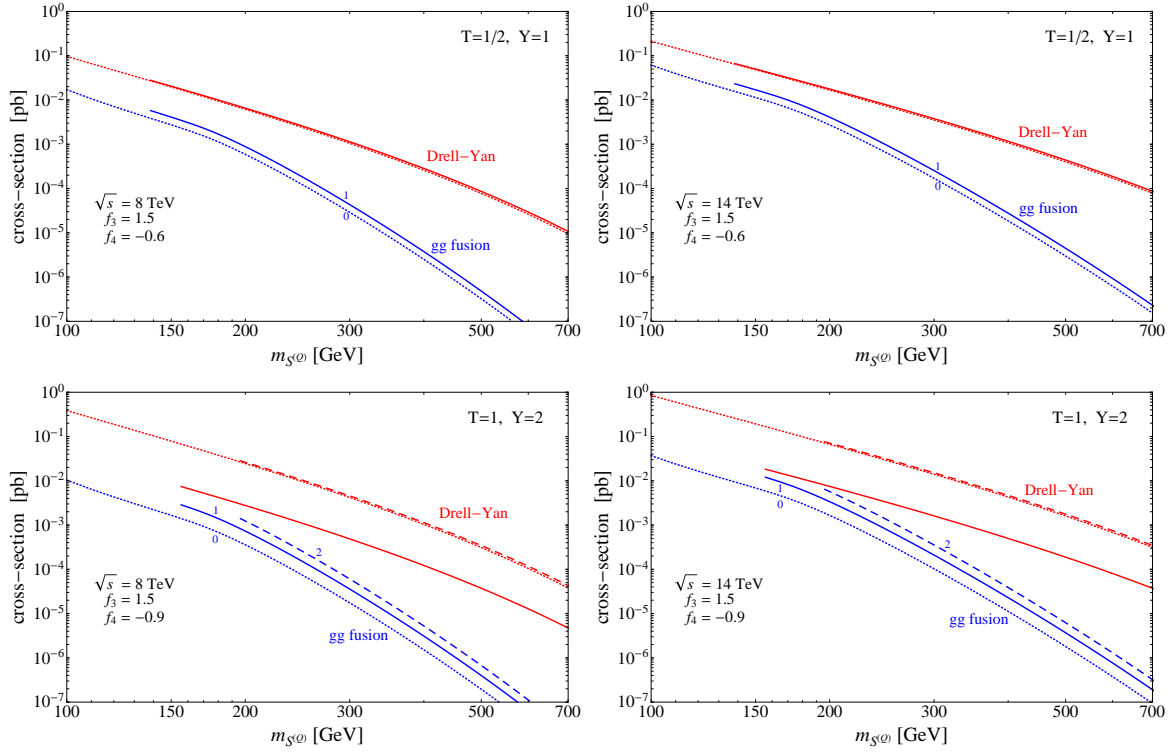


Figure 2: Gluon-gluon fusion and Drell-Yan production cross-sections for two different representations of $SU(2)_L$. The dashed, solid and dotted lines correspond to the production of scalars with electric charge equal to +2, +1 and 0, respectively. For the doublet, the effective couplings are $\Lambda_{+1} = -3.3$, $\Lambda_0 = -2.7$ and, for the triplet, $\Lambda_{+2} = -3.9$, $\Lambda_{+1} = -3$ and $\Lambda_0 = -2.1$.

scalar mass changes when $m_{S(Q)} \simeq m_t$, which is due to the different functional form of the Higgs coupling with gluons when the partonic center-of-mass energy is larger or smaller than the top mass, see Eq. (3). Moreover, we find that for the electrically neutral component of the multiplet, the ratio $\sigma_{\text{ggF}}\Lambda_Q^{-2}/\sigma_{\text{DY}}$ decreases as the isospin increases. Nevertheless, due to the complicated dependence of the Drell-Yan cross-section with the electric charge and the hypercharge, it is not possible to ascertain a pattern within the members of the same multiplet.

More specifically, we show in Fig. 2 the scalar production cross-sections associated with the ggF (blue lines) and DY (red lines) sub-processes for fixed values of the quartic couplings f_3 and f_4 . We consider two specific scenarios: *i*) doublet with $Y = 1$ (upper panels) and *ii*) triplet with $Y = 2$ (lower panels). We have checked that for this choice of quantum numbers the couplings are in agreement with the constraints on the parameter space discussed earlier in this section. The dashed, solid and dotted lines correspond to the production of scalars with electric charge equal to +2, +1 and 0, respectively. Notice

that Eq. (15) sets a lower bound on the mass of each component of the multiplet, which has been taken into account for the mass range depicted in Fig. 2. In the shown mass range, the $h \rightarrow \gamma\gamma$ signal strength is consistent with the CMS measurement [29] at the 2σ level, while the T parameter does not deviate from the best fit value [30] by more than 1σ . We find, in particular, that the production cross-section of the neutral and charged component of the doublet is approximately a factor 5 (2) smaller than the corresponding Drell-Yan cross-section for $m_{S(Q)} \simeq 140$ GeV and c.o.m. energy of 8 (14) TeV. For the scalar triplet, the gluon-gluon fusion and Drell-Yan production cross-sections of the singly charged component differ by a factor smaller than 4 (2) for $m_{S(+1)} \lesssim 180$ GeV at 8 (14) TeV, while electroweak interactions provide clearly the dominant contribution to the production of the neutral and doubly charged scalars, within all the mass range.

4 Fermion production at the LHC

We consider in this section the impact of the gluon-gluon fusion mechanism on the production of new fermionic representations at the LHC. In what follows we assume a simplified scenario with just one extra uncoloured fermion multiplet ψ , which has Yukawa-type interactions involving the Higgs doublet and the SM leptons L, E :⁶

$$\mathcal{L}_\psi = c\bar{\psi}(i\not{D} - m_\psi)\psi + \mathcal{L}_Y(H, \psi, L, E), \quad (23)$$

where c is a constant which equals 1 (1/2) if ψ is a Dirac (Majorana) fermion. Depending on the quantum number assignments, such an interaction may or may not exist at the renormalizable level. The spontaneous breaking of the electroweak symmetry results in an interaction between the Higgs boson and the new fermionic mass eigenstate(s), as well as a mixing between SM lepton flavours and the new fermion(s), which can be sizeable depending on the details of the model. The requirement of renormalizability of Lagrangian (23) restricts our analysis to the case in which the new fermion ψ has zero hypercharge and is either a singlet or a triplet of $SU(2)_L$, as in the well known type I [5] and type III [6] seesaw extensions of the SM. Here, we have additional heavy right-handed Majorana neutrinos which mix with the SM left-handed neutrinos. The mixing between the heavy and light neutrinos can be encoded in a matrix $\Theta_{\alpha k}$, which enters the expression of the light neutrino mass matrix, $(m_\nu)_{\alpha\beta} = \Theta_{\alpha k}^* M_k \Theta_{k\beta}^\dagger$. The matrix elements of $\Theta_{\alpha k}$ are constrained by lepton flavour violating processes, notably by $\mu \rightarrow e \gamma$. Typically, $|\Theta_{\alpha k}| \lesssim 10^{-2}$ in the type I seesaw for a heavy neutrino mass $M \sim 100$ GeV, whereas the type III requires smaller values for $|\Theta_{\alpha k}|$ [34].

⁶A simple interesting alternative are models with vector-like fermions, see e.g. [31] and [32]. For an analysis of the impact of gluon-gluon fusion in these models, see [33].

We discuss in this framework the production of heavy Majorana fermions, \mathcal{N}_k , and charged Dirac fermions, \mathcal{E}_k , with a mass M_k varying in the electroweak range (see, *e.g.*, [34] for a phenomenological analysis of such seesaw scenarios). The production proceeds either through the Drell-Yan processes or through the gluon-gluon fusion mechanism involving a Higgs and a Z , as discussed in section 2. For a collider signal analysis of the far stronger channels $q\bar{q}' \rightarrow W^* \rightarrow \mathcal{N}\ell^\pm$ for type I and $q\bar{q} \rightarrow Z^* \rightarrow \mathcal{E}^+\mathcal{E}^-$, $q\bar{q}' \rightarrow W^* \rightarrow \mathcal{E}^\pm\mathcal{N}$ for type III, see, *e.g.*, [8]. These channels are not considered here because either the final state cannot be obtained via a Higgs-mediated process, or it is suppressed by a higher power of the mixing parameter.

In the particular case of heavy Majorana neutrinos, \mathcal{N}_k ($k = 1, 2, \dots$), involved in the generation of active neutrino masses through the type I/III seesaw mechanism, the relevant couplings to the Z and the Higgs boson after electroweak symmetry breaking can be parametrized by the following effective Lagrangian terms

$$\mathcal{L}_{NC}^{\mathcal{N}} = -\frac{g}{4c_w} \bar{\nu}_{\alpha L} \gamma_\mu \Theta_{\alpha k} (1 - \gamma_5) \mathcal{N}_k Z^\mu + \text{h.c.}, \quad (24)$$

$$\mathcal{L}_H^{\mathcal{N}} = -\frac{g M_k}{4 m_W} \bar{\nu}_{\alpha L} \Theta_{\alpha k} (1 + \gamma_5) \mathcal{N}_k h + \text{h.c.}, \quad (25)$$

where M_k is the mass of the k th heavy Majorana neutrino and m_W denotes the W boson mass.

In the type III seesaw scenario, the SM Lagrangian is extended with new fermionic representations in the adjoint of the weak gauge group. As a consequence, there exists for each Majorana neutrino \mathcal{N}_k one Dirac fermion \mathcal{E}_k with electric charge -1 and degenerate in mass with \mathcal{N}_k at leading order. These new heavy charged fermions are coupled to the electroweak gauge bosons and the SM leptons through the mixing matrix $\Theta_{\alpha k}$:

$$\mathcal{L}_{NC}^{\mathcal{E}} = -\frac{g}{2\sqrt{2}c_w} \bar{\ell}_\alpha \gamma_\mu \Theta_{\alpha k} (1 - \gamma_5) \mathcal{E}_k Z^\mu + \text{h.c.} \quad (26)$$

Similarly, the coupling of \mathcal{E}_j and the Higgs boson is parametrized by the interaction Lagrangian

$$\mathcal{L}_H^{\mathcal{E}} = -\frac{g M_k}{2\sqrt{2}m_W} \bar{\ell}_\alpha \Theta_{\alpha k} (1 + \gamma_5) \mathcal{E}_k h + \text{h.c.} \quad (27)$$

We consider now the possibility of producing heavy fermionic states in the framework of the low-scale seesaw scenario. The relevant interactions for the production through the ggH portal are given in Eqs. (25) and (27). Away from the Higgs resonance and neglecting the mass of the SM leptons, we obtain for the production cross-section via an intermediate Higgs boson:

$$\sigma_H(gg \rightarrow \mathcal{N}_k \nu_\alpha; \hat{s}) = \sigma_H(gg \rightarrow \mathcal{E}_k \bar{\ell}_\alpha; \hat{s}) = \frac{\pi \alpha_{\text{em}}^2 |\Theta_{\alpha k}|^2 G_H^2 M_k^2 (M_k^2 - \hat{s})^2}{512 s_w^4 c_w^4 m_Z^2 (m_h^2 - \hat{s})^2}, \quad (28)$$

where the effective gluon-gluon-Higgs coupling G_H is given in Eq. (2). Notice that, for fermion masses M_k below the Higgs boson mass, the corresponding \mathcal{N}_k or \mathcal{E}_k production cross-section is resonantly enhanced.

On the other hand, the relevant interactions for the neutral current interactions are given in Eqs. (24) and (26). The partonic production cross-section of one heavy fermion and one massless SM lepton via the ggZ interaction reads

$$\begin{aligned}\sigma_Z(gg \rightarrow \mathcal{N}_k \nu_\alpha; \hat{s}) &= \sigma_Z(gg \rightarrow \mathcal{E}_k \ell_\alpha; \hat{s}) \\ &= \frac{\alpha_{\text{em}} |\Theta_{\alpha k}|^2 G_Z^2 M_k^2 \hat{s}^2 \left(1 - \frac{M_k^2}{\hat{s}}\right)^2}{2048 s_w^2 c_w^2 m_Z^4},\end{aligned}\quad (29)$$

where G_Z is given in Eq. (6). As mentioned in section 2, we only consider the top quark contribution. Note also the absence of a resonance in $\hat{s} = m_Z^2$ due to the Landau-Yang theorem [35]: an on-shell Z boson cannot be produced in the collision of two massless spin-1 vector bosons.

Lastly, the expressions for the production cross-section in a quark-antiquark collision read:

$$\begin{aligned}\sigma(u\bar{u} \rightarrow \mathcal{N}_k \nu_\alpha; \hat{s}) &= \sigma(u\bar{u} \rightarrow \mathcal{E}_k \bar{\ell}_\alpha; \hat{s}) \\ &= \frac{\pi \alpha_{\text{em}}^2 |\Theta_{\alpha k}|^2 (\hat{s} - M_k^2)^2 (M_k^2 + 2\hat{s})}{1296 c_w^4 s_w^4 (\hat{s} - m_Z^2)^2 \hat{s}^2} (9 c_w^4 - 6 c_w^2 s_w^2 + 17 s_w^4),\end{aligned}\quad (30)$$

$$\begin{aligned}\sigma(d\bar{d} \rightarrow \mathcal{N}_k \nu_\alpha; \hat{s}) &= \sigma(d\bar{d} \rightarrow \mathcal{E}_k \bar{\ell}_\alpha; \hat{s}) \\ &= \frac{\pi \alpha_{\text{em}}^2 |\Theta_{\alpha k}|^2 (\hat{s} - M_k^2)^2 (M_k^2 + 2\hat{s})}{1296 c_w^4 s_w^4 (\hat{s} - m_Z^2)^2 \hat{s}^2} (9 c_w^4 + 6 c_w^2 s_w^2 + 5 s_w^4).\end{aligned}\quad (31)$$

The total fermion production cross-section at the LHC, for a c.o.m. energy \sqrt{s} , is given by the convolution of the corresponding cross-section, Eqs. (28-31), with the corresponding parton luminosity functions, as described in Eqs. (8-11) and taking $\tau_s \equiv M_k^2/s$ in the limit of massless charged leptons.

We report in Fig. 3, left panel, the ratio between the gluon-gluon fusion and the Drell-Yan production cross-sections of a Majorana neutrino \mathcal{N}_1 or charged fermion \mathcal{E}_1 as a function of the fermion mass M_1 . The two curves correspond to the LHC c.o.m. energy of 8 TeV (dashed line) and 14 TeV (continuous line), respectively. Notice that, at lowest order in the mixing parameter, the ratio of σ_{ggF} and σ_{DY} for these final states does not depend on the mixing between heavy fermions and SM leptons. We also report on the right panel the production cross-sections for a fixed value of the mixing parameter, $|\Theta_{\alpha 1}| = 10^{-2}$, and $\sqrt{s} = 14$ TeV. As apparent from the plot, the (Higgs-mediated) gluon-

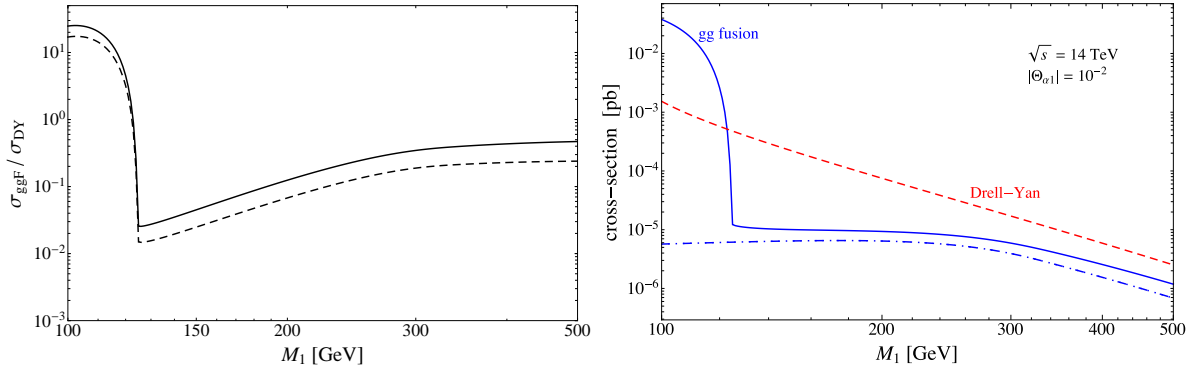


Figure 3: *Left panel:* ratio between gluon-gluon fusion and Drell-Yan production cross-sections of heavy fermions in type I/III seesaw scenarios at $\sqrt{s} = 8$ (14) TeV, dashed (continuous) line. *Right panel:* Fermion production cross-sections for $\sqrt{s} = 14$ TeV and $|\Theta_{\alpha 1}| = 10^{-2}$. The solid blue line represents the complete contribution due to gluon-gluon fusion, while the dot-dashed blue line shows the contribution from ggZ alone.

gluon fusion vertex provides the largest contribution to the fermion production cross-section for masses $M_k \lesssim m_h$, due to the resonant enhancement for fermion masses below the Higgs pole. This opens the possibility of testing the type I scenario at the energy frontier via Higgs boson exotic decays. For example, the production and detection of the heavy Majorana fermions might be feasible via the chain $h \rightarrow \nu_{\alpha L} N_j$, with $N_j \rightarrow \ell_\beta W, \nu Z$ and the gauge bosons subsequently decaying producing jets or leptons (see [36, 37] for detailed discussions about these signals at the LHC). On the other hand, for larger heavy fermion masses the gluon-gluon fusion process only gives a subdominant contribution to the total production cross-section, although this contribution can be as large as 40%-50% for $\sqrt{s} = 14$ TeV and should not be neglected. This is the case, in particular, of the type III seesaw, where the extra fermion masses are restricted to be $m_{\mathcal{N}} \gtrsim 300$ GeV, as follows from the ATLAS search for the final state \mathcal{EN} presented in [38].

5 Perspectives for a $\sqrt{s} = 100$ TeV proton-proton collider

There is currently a growing discussion within the Particle Physics community regarding the first steps towards the post-LHC era. In particular, the planning of future high energy facilities is a long term endeavour and requires careful consideration of the expected physics opportunities. In this context, it is timely to assess the impact of the gluon-

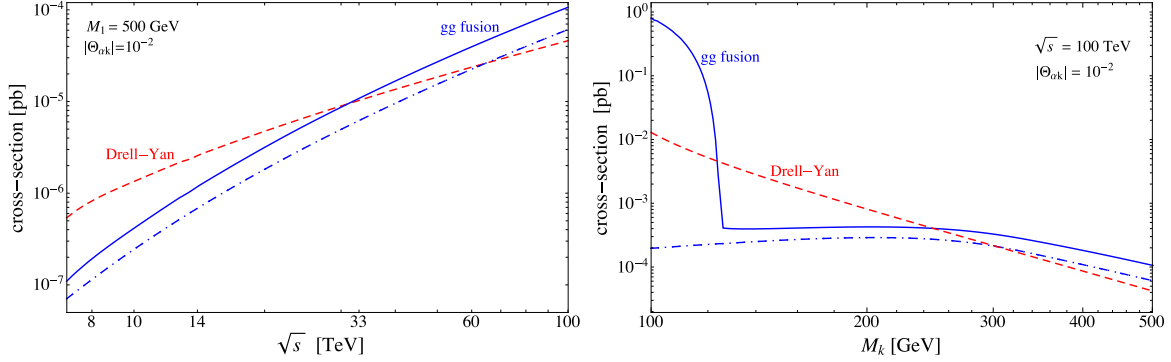


Figure 4: *Left panel:* Cross-section for the production of an $\mathcal{E}_k \ell_\alpha$ or $\mathcal{N}_k \nu_\alpha$ pair with $|\Theta_{\alpha k}| = 10^{-2}$ both from Drell-Yan and gluon-gluon fusion for varying \sqrt{s} . *Right panel:* Fermion production cross-sections for $\sqrt{s} = 100$ TeV and $|\Theta_{\alpha k}| = 10^{-2}$ as a function of M_k .

gluon fusion mechanism on the production rate of new particles beyond the SM at future machines, such as a high energy upgrade of the LHC with 33 TeV center-of-mass energy [39] or a hypothetical 100 TeV proton-proton collider [40]. In the following, we will concentrate our discussion mostly on the latter possibility.

We consider for concreteness the production of a charged component of a fermionic triplet \mathcal{E}_k with mass $M_k = 500$ GeV and a mixing parameter $|\Theta_{\alpha k}| = 10^{-2}$, in association with a SM fermion ℓ_α . As can be seen in Fig. 4, left panel, a higher center-of-mass energy has two main effects on the cross-section. First, a larger value of \sqrt{s} at a hadron collider implies a larger cross-section for both Drell-Yan and the gluon-gluon fusion mechanism, since parton luminosities increase and a larger multi-body phase space becomes available. Second, the relative importance of different partons changes, thus leading to both more flavour democratic contributions to Drell-Yan as well as an increasing relevance of gluon initial states. For this exemplary case, the relative importance of the gluon-gluon fusion increases by one order of magnitude and hence the gluon-gluon fusion cross-section σ_{ggF} becomes as important as the Drell-Yan contribution σ_{DY} at $\sqrt{s} = 30$ TeV and is completely dominant at $\sqrt{s} = 100$ TeV, as shown in Fig. 4 (left panel). More specifically, and as apparent from Fig. 4 (right panel), for a 100 TeV proton-proton collider the gluon-gluon fusion contribution is the dominant production channel for the range of masses currently allowed by the ATLAS search of the charged component of the fermionic triplet [38], $M_k \gtrsim 300$ GeV. Interestingly, with a proposed luminosity of up to $L = 10 \text{ ab}^{-1}$, hundreds of events can be expected, provided $M_k \lesssim 500$ GeV.

Qualitatively, the impact on the scalar production is similar, as we find an increase of the gluon-gluon fusion cross-section $\sigma_{\text{ggF}}(100 \text{ TeV})$ by two orders of magnitude compared

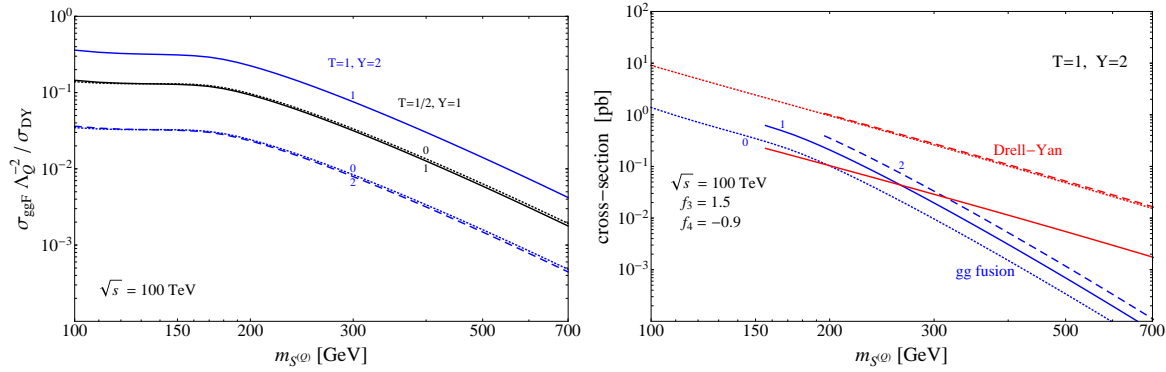


Figure 5: *Left panel:* Ratio between Higgs-mediated and Drell-Yan production cross-sections of a scalar triplet at $\sqrt{s} = 100$ TeV. *Right panel:* Scalar triplet production cross-sections with parameters as in Fig. 2 for $\sqrt{s} = 100$ TeV

to $\sigma_{\text{ggF}}(14 \text{ TeV})$ and a sizeable increase with respect to the DY process. As can be seen in Fig. 5, the larger gluon luminosity can render the gluon-gluon fusion mechanism dominant for the singly charged component of a scalar triplet, with couplings equal to the ones in Fig. 2, up to scalar masses of 260 GeV. Furthermore, one expects exotic scalars to be copiously produced at a 100 TeV collider with a luminosity of 10 ab^{-1} . More specifically, we estimate that at least 10^7 to 10^4 pairs of singly charged scalars can be produced for masses in the range 100 to 700 GeV, even if Λ_Q should happen to be small.

6 Conclusions

We have investigated in this work the production of exotic fermions and scalars at the Large Hadron Collider via gluon-gluon fusion, in scenarios where the extra states couple to the SM Higgs boson. More concretely, we have studied extensions of the SM by just one complex scalar field or by one fermionic field. The gauge symmetry does not restrict the gauge quantum numbers of the scalar field, while the fermionic field must be either a singlet or a $SU(2)_L$ triplet with no hypercharge and no colour, as in the type I and type III seesaw mechanisms, respectively. In many of these scenarios, then, the extra states have also electroweak interactions and can be produced by the Drell-Yan process with the mediation of a photon or a Z boson. For the production of exotic scalar particles, we have found that the Higgs-mediated processes can give sizeable contributions to the total cross-section when the quartic couplings are $\gtrsim \mathcal{O}(1)$, which can be comparable to the QCD or electroweak corrections. On the other hand, for the production of exotic

fermionic particles, the relative size of both contributions does not depend on the Yukawa coupling in the minimal scenario considered in this work. We find for this case that the Higgs-mediated channel dominates the production when the mass of the fermion is $\lesssim 120$ GeV. Lastly, motivated by the current discussions on the physics opportunities at future proton-proton colliders, we have briefly addressed the prospects to produce new exotic scalars and fermions in this hypothetical machine. We find that, in general, the Higgs interaction gives a non-negligible contribution to the total production cross-section and that the gluon-gluon fusion constitutes the dominant contribution to the production of heavy fermions at $\sqrt{s} = 100$ TeV.

Acknowledgments

The work of A. I. and E. M. is supported by the ERC Advanced Grant project “FLAVOUR” (267104). This work has been partially supported by the DFG cluster of excellence “Origin and Structure of the Universe”. S. V. also acknowledges support from the DFG Graduiertenkolleg “Particle Physics at the Energy Frontier of New Phenomena”. A. G. H. is supported by Fundação para a Ciência e a Tecnologia (FCT) through the grant SFRH/BD/76052/2011, financed by the European Social Fund (ESF) through POPH under the QREN framework.

References

- [1] G. Aad *et al.* [ATLAS Collaboration], Phys. Lett. B **716** (2012) 1 [arXiv:1207.7214 [hep-ex]].
- [2] S. Chatrchyan *et al.* [CMS Collaboration], Phys. Lett. B **716** (2012) 30 [arXiv:1207.7235 [hep-ex]].
- [3] CMS Collaboration [CMS Collaboration], and studies of the compatibility of its couplings with the standard model,” CMS-PAS-HIG-14-009.
- [4] J. Alcaraz *et al.* [ALEPH and DELPHI and L3 and OPAL and LEP Electroweak Working Group Collaborations], arXiv:0712.0929 [hep-ex].
- [5] P. Minkowski, Phys. Lett. B **67** (1977) 421; M. Gell-Mann, P. Ramond and R. Slansky, *Proceedings of the Supergravity Stony Brook Workshop*, New York 1979, eds. P. Van Nieuwenhuizen and D. Freedman; T. Yanagida, *Proceedings of the Workshop on Unified Theories and Baryon Number in the Universe*, Tsukuba, Japan 1979,

- eds. A. Sawada and A. Sugamoto; R. N. Mohapatra and G. Senjanovic, Phys. Rev. Lett. **44** (1980) 912.
- [6] R. Foot, H. Lew, X. G. He and G. C. Joshi, Z. Phys. C **44** (1989) 441. E. Ma, Phys. Rev. Lett. **81** (1998) 1171 [arXiv:hep-ph/9805219].
 - [7] F. del Aguila and L. Ametller, Phys. Lett. B **261** (1991) 326.
 - [8] F. del Aguila and J. A. Aguilar-Saavedra, Nucl. Phys. B **813** (2009) 22 [arXiv:0808.2468 [hep-ph]].
 - [9] R. Franceschini, T. Hambye and A. Strumia, Phys. Rev. D **78** (2008) 033002 [arXiv:0805.1613 [hep-ph]].
 - [10] M. Spira, A. Djouadi, D. Graudenz and P. M. Zerwas, Nucl. Phys. B **453** (1995) 17 [hep-ph/9504378].
 - [11] A. Djouadi, Phys. Rept. **457** (2008) 1 [hep-ph/0503172].
 - [12] T. Plehn, M. Spira and P. M. Zerwas, Nucl. Phys. B **479** (1996) 46 [Erratum-ibid. B **531** (1998) 655] [hep-ph/9603205].
 - [13] J. S. Bell and R. Jackiw, Il Nuovo Cimento A **60** (1969), 47
 - [14] D. A. Dicus and P. Roy, Phys. Rev. D **44** (1991), 1593
 - [15] <https://twiki.cern.ch/twiki/bin/view/LHCPhysics/CrossSections>
 - [16] T. Hambye, F. -S. Ling, L. Lopez Honorez and J. Rocher, JHEP **0907** (2009) 090 [Erratum-ibid. **1005** (2010) 066] [arXiv:0903.4010 [hep-ph]].
 - [17] K. Hally, H. E. Logan and T. Pilkington, Phys. Rev. D **85** (2012) 095017 [arXiv:1202.5073 [hep-ph]]. K. Earl, K. Hartling, H. E. Logan and T. Pilkington, Phys. Rev. D **88** (2013) 015002 [arXiv:1303.1244 [hep-ph]].
 - [18] M. B. Einhorn, D. R. T. Jones, M. Veltman, Nucl. Phys. D **191** 1 (1981) 146. M. E. Peskin, T. Takeuchi, Phys. Rev. Lett. **65** (1990) 964. M. E. Peskin, T. Takeuchi, Phys. Rev. D **46** (1992) 381.
 - [19] L. Lavoura and L. F. Li, Phys. Rev. D **49** (1994) 1409 [hep-ph/9309262].
 - [20] J. F. Gunion, H. E. Haber, G. L. Kane and S. Dawson, Front. Phys. **80** (2000) 1.
 - [21] M. Cirelli, N. Fornengo and A. Strumia, Nucl. Phys. B **753** (2006) 178 [hep-ph/0512090].

- [22] E. Ma, Phys. Rev. Lett. **86** (2001) 2502 [hep-ph/0011121].
- [23] W. Grimus, L. Lavoura and B. Radovic, Phys. Lett. B **674** (2009) 117 [arXiv:0902.2325 [hep-ph]].
- [24] F. -X. Josse-Michaux and E. Molinaro, Phys. Rev. D **84** (2011) 125021 [arXiv:1108.0482 [hep-ph]]; F. -X. Josse-Michaux and E. Molinaro, Phys. Rev. D **87** (2013) 3, 036007 [arXiv:1210.7202 [hep-ph]].
- [25] M. Magg and C. Wetterich, Phys. Lett. B **94** (1980) 61; J. Schechter and J. W. F. Valle, Phys. Rev. D **22** (1980) 2227; R. N. Mohapatra and G. Senjanovic, Phys. Rev. D **23** (1981) 165.
- [26] A. G. Akeroyd, S. Moretti and H. Sugiyama, Phys. Rev. D **85** (2012) 055026 [arXiv:1201.5047 [hep-ph]].
- [27] A. Belyaev, N. D. Christensen and A. Pukhov, Comput. Phys. Commun. **184** (2013) 1729 [arXiv:1207.6082 [hep-ph]].
- [28] J. Pumplin, D. R. Stump, J. Huston, H. L. Lai, P. M. Nadolsky and W. K. Tung, JHEP **0207** (2002) 012 [hep-ph/0201195].
- [29] CMS Collaboration [CMS Collaboration], CMS-PAS-HIG-13-016.
- [30] M. Baak, J. Cuth, J. Haller, A. Hoecker, R. Kogler, K. Moenig, M. Schott and J. Stelzer, arXiv:1407.3792 [hep-ph].
- [31] A. Delgado, C. Garcia Cely, T. Han and Z. Wang, Phys. Rev. D **84** (2011), 073007 [arXiv:1105.5417 [hep-ph]]
- [32] T. Ma, Z. Bin and G. Cacciapaglia, Phys. Rev. D **89** (2014), 093022 [arXiv:1404.2375 [hep-ph]]
- [33] C. Liu and S. Yang, Phys. Rev. D **81** (2010), 093009 [arXiv:1005.1362 [hep-ph]]
- [34] A. Ibarra, E. Molinaro and S. T. Petcov, JHEP **1009** (2010) 108 [arXiv:1007.2378 [hep-ph]]. A. Ibarra, E. Molinaro and S. T. Petcov, Phys. Rev. D **84** (2011) 013005 [arXiv:1103.6217 [hep-ph]]. D. N. Dinh, A. Ibarra, E. Molinaro and S. T. Petcov, JHEP **1208** (2012) 125 [arXiv:1205.4671 [hep-ph]].
- [35] L. D. Landau, Dokl. Akad. Nauk., USSR **60** (1948), 207; C. N. Yang, Phys. Rev. **77** (1950), 242

- [36] C. G. Cely, A. Ibarra, E. Molinaro and S. T. Petcov, Phys. Lett. B **718** (2013) 957 [arXiv:1208.3654 [hep-ph]].
- [37] P. S. Bhupal Dev, R. Franceschini and R. N. Mohapatra, Phys. Rev. D **86** (2012) 093010 [arXiv:1207.2756 [hep-ph]].
- [38] [ATLAS Collaboration], ATLAS-CONF-2013-019.
- [39] E. Todesco and F. Zimmermann, arXiv:1111.7188 [physics.acc-ph].
- [40] BSM physics opportunities at 100 TeV, <http://indico.cern.ch/event/284800/overview>.